Energy Conversion and Management 50 (2009) 2768–2781

Contents lists available at ScienceDirect

Energy Conversion and Management

journal homepage: www.elsevier.com/locate/enconman

Thermoeconomic analysis of a novel zero-CO_2-emission high-efficiency power cycle using LNG coldness

Meng Liu [a], Noam Lior [c,*], Na Zhang [b], Wei Han [b]

[a] China National Institute of Standardization, Beijing 100088, PR China
[b] Institute of Engineering Thermophysics, Chinese Academy of Sciences, P.O. Box 2706, Beijing 100190, PR China
[c] Department of Mechanical Engineering and Applied Mechanics, University of Pennsylvania, Philadelphia, PA 19104-6315, USA

ARTICLE INFO

Article history:
Received 30 November 2008
Accepted 29 June 2009
Available online 12 August 2009

Keywords:
Oxy-fuel power system
LNG
Coldness energy
Power generation
Thermoeconomics
CO_2 capture

ABSTRACT

This paper presents a thermoeconomic analysis aimed at the optimization of a novel zero-CO_2 and other emissions and high-efficiency power and refrigeration cogeneration system, COOLCEP-S (Patent pending), which uses the liquefied natural gas (LNG) coldness during its revaporization. It was predicted that at the turbine inlet temperature (*TIT*) of 900 °C, the energy efficiency of the COOLCEP-S system reaches 59%. The thermoeconomic analysis determines the specific cost, the cost of electricity, the system payback period and the total net revenue. The optimization started by performing a thermodynamic sensitivity analysis, which has shown that for a fixed *TIT* and pressure ratio, the pinch point temperature difference in the recuperator, ΔT_{p1}, and that in the condenser, ΔT_{p2} are the most significant unconstrained variables to have a significant effect on the thermal performance of novel cycle. The payback period of this novel cycle (with fixed net power output of 20 MW and plant life of 40 years) was ~5.9 years at most, and would be reduced to ~3.1 years at most when there is a market for the refrigeration byproduct. The capital investment cost of the economically optimized plant is estimated to be about 1000 $/kWe, and the cost of electricity is estimated to be 0.34–0.37 CNY/kWh (~0.04 $/kWh). These values are much lower than those of conventional coal power plants being installed at this time in China, which, in contrast to COOLCEP-S, do produce CO_2 emissions at that.

1. Introduction

Natural gas is one of the most widely used fossil energy resource with higher heat value and less pollutant production than the other fossil energy resources. Since the first liquefied natural gas (LNG) trade in 1964, the global LNG trade has seen a continuously rapid growth, mainly because the transformation from natural gas to the LNG reduces its volume by about 600-fold and thus facilitates the conveyance from the gas source to receiving terminal. Liquefaction of the gas to LNG requires, however, approximately 500 kWh electric energy per ton LNG, It is noteworthy that the LNG, at about 110 K, thus contains a considerable portion of the energy and exergy that were invested in this process. The principle of the novel COOLCEP-S system is the effective use of that stored potential during the revaporization and heating to approximately ambient temperature of the LNG for pipeline transmission to the consumers. This use of the valuable energy and exergy replaces the commonly employed revaporization methods of using ambient (ocean or air) or gas combustion heat, which simply waste it and may also cause undesirable environmental effects.

Recovery of the cryogenic exergy in the LNG evaporation process by incorporating this process into a properly designed thermal power cycle, in different ways, has been proposed in a number of past publications [1–13]. This includes methods which use the LNG as the working fluid in natural gas direct expansion cycles, or its coldness as the heat sink in closed-loop Rankine cycles [1–6], Brayton cycles [7–9], and combinations thereof [10,11]. Other methods use the LNG coldness to improve the performance of conventional thermal power cycles. For example, LNG vaporization can be integrated with gas turbine inlet air cooling [5,12] or steam turbine condenser system (by cooling the recycled water [11]), etc. Some pilot plants have been established in Japan from the 1970s, combining closed-loop Rankine cycles (with pure or mixture organic working fluids) and direct expansion cycles [1].

Increasing concern about greenhouse effects on climate change prompted a significant growth in research and practice of CO_2 emission mitigation in recent years. The main technologies proposed for CO_2 capture in power plants are physical and chemical absorption, cryogenic fractionation, and membrane separation. The amount of energy needed for the CO_2 capture would lead to the reduction of power generation energy efficiency by up to 10 percentage points [14,15].

* Corresponding author.
E-mail addresses: liumeng@cnis.gov.cn (M. Liu), lior@seas.upenn.edu (N. Lior).

0196-8904/$ - see front matter © 2009 Elsevier Ltd. All rights reserved.
doi:10.1016/j.enconman.2009.06.033

Beside the efforts for reduction of CO_2 emissions from existing power plants, concepts of power plants having zero-CO_2-emission were proposed and studied. Oxy-fuel combustion is one of the proposed removal strategies. It is based on the close-to-stoichiometric combustion, where the fuel is burned with enriched oxygen (produced in an air separation unit, ASU) and recycled flue gas. The combustion is accomplished in absence of the large amounts of nitrogen and produces only CO_2 and H_2O. CO_2 separation is accomplished by condensing water from the flue gas and therefore requires only a modest amount of energy. Some of the oxy-fuel cycles with ASU and recycled CO_2/H_2O from the flue gas are the Graz cycle, the Water Cycle, and the Matiant cycle [16–20]. We proposed and analyzed the semi-closed oxy-fuel cycles with integration of the LNG cold exergy utilization [21,22]. The additional power use for O_2 production amounts to 7–10% of the cycle total input energy. To reduce the oxygen production efficiency penalty, new technologies have been developed, such as chemical looping combustion (CLC) [23,24] and the AZEP concept [25], employing, respectively, oxygen transport particles and membranes to separate O_2 from air. Kvamsdal et al. [26] made a quantitative comparison of various cycles with respect to plant efficiency and CO_2 emissions, and concluded that the adoption of these new technologies shows promising performance because no additional energy is then necessary for oxygen separation, but they are still under development.

We proposed and analyzed a novel zero-CO_2-emission power cycle using LNG coldness, with the name of COOLCEP-S [27], which is based on the concept proposed by Deng et al. [6]: that is a cogeneration (power and refrigeration) recuperative Rankine cycle with CO_2 as the main working fluid. Combustion takes place with natural gas burning in an oxygen and recycled-CO_2 mixture. The high turbine inlet temperature and turbine exhaust heat recuperation present a high heat addition temperature level, and the heat sink at a temperature lower than the ambient accomplished by heat exchange with LNG offer high power generation efficiency. At the same time, these low temperatures allow condensation of the working fluid and the combustion-generated CO_2 is thus captured. Furthermore, the sub-critical re-evaporation of the CO_2 working fluid is accomplished below ambient temperature and can thus provide refrigeration if needed.

The primary advances over the work presented in [6] are the integration of the LNG evaporation with the CO_2 condensation and capture. In the analysis in [6], it was assumed that LNG consists of pure CH_4 and the combustion production after water removal can be fully condensed at the 5.3 bar/−53.1 °C. In COOLCEP-S, we used a different condensation process: first the amount of the working fluid needed for sustaining the process is condensed and recycled, and the remaining working fluid, having a relatively small mass flow rate (<5% of the total turbine exhaust flow rate after water removal) and higher concentration of noncondensable gases, are compressed to a higher pressure level and then condensed. Alternatively, the CO_2-enriched flue gas can be condensed at a lower temperature, which can be provided by the LNG coldness, but it would then freeze the CO_2 and is thus not considered in this paper; instead we adopted a higher condensation pressure for the flue stream condensation, which leads to a more conservative solution and some efficiency penalty but can recover the CO_2 fully. It is found that, at the turbine inlet temperature of 900 °C and the pressure ratio of four, the energy efficiency of the COOLCEP-S cycle reaches 59%.

In this study we performed a thermoeconomic analysis of that system, to determine the conditions and costs for optimal system operation and configuration. A much more limited paper on the subject was presented as [28].

Consider the thermoeconomic analysis, the recuperator and the CO_2 condenser are the two most important heat exchangers in the COOLCEP-S cycle in their effect on performance and cost. In this paper, we conduct a thermoeconomic optimization of the pinch point temperature differences, the ΔT_{p1} in the recuperator and the ΔT_{p2} in the CO_2 condenser, based on the cycle thermal and exergy efficiencies, and the economic performance evaluation criteria that include the plant specific cost, the cost of electricity, the payback period and the total net revenue, to find the thermoeconomically optimal values of ΔT_{p1} and ΔT_{p2}.

2. System configuration description

Fig. 1 shows the layout of the COOLCEP-S cycle, which consists of a power subcycle and an LNG vaporization process. Fig. 2 is the cycle *t–s* diagram. The interfaces between the power subcycle and the LNG vaporization process are the CO_2 condenser CON, the heat exchangers HEX1, and the fuel feed stream 8.

The power subcycle can be identified as 1-2-3-4-5-6-7-8-9-10-11-12/13-14-1. The low temperature (−50 °C) liquid CO_2 as the main working fluid (1) is pumped to about 30 bar (2), then goes through a heat addition process (2−3) in the evaporator EVA1 and can thereby produce refrigeration if needed. The O_2 (4) produced in an air separator unit (ASU) is compressed and mixed with the main CO_2 working fluid. The gas mixture (6) is heated (6–7) by turbine (GT) exhaust heat recuperation in REP. The working fluid temperature is further elevated in the combustor B, fueled with natural gas (8), to its maximal value (the turbine inlet temperature *TIT*) (9). The working fluid expands to the working fluid condensation pressure (10) in the gas turbine (GT) to generate power and is then cooled (to 11) in the recuperator REP.

The gases in the mixture at the exit of REP (11) need to be separated, and the combustion-generated CO_2 component needs to be condensed for ultimate sequestration, and this is performed by further cooling: in the LNG-cooled heat exchanger HEX1, in which the H_2O vapor in the mixture is condensed and drained out (12). Afterwards, the remaining working gas (13) is condensed (14) in the condenser CON against the LNG evaporation, and recycled (1). The remaining working fluid (15) enriched with noncondensable species (mainly N_2, Ar and O_2) is further compressed in C3 to a higher pressure level under which the combustion-generated CO_2 is condensed and captured, ready for final disposal.

The LNG vaporization process is 18-19-19a/b-20a/b-20-21-22-23/8. LNG (18) is pumped by P2 to the highest pressure (73.5 bar), typical for receiving terminals which supply long distance pipeline network, and then evaporated with the heat addition from the power cycle. The evaporated NG (natural gas) may produce a small amount of cooling in HEX3 if its temperature is still low enough at the exit of HEX1, and thus contribute to the overall system useful outputs. Finally, the emerging natural gas stream is split into two parts where most of it (23) is sent to outside users and a small part (8) is used as the fuel in the combustor of this cycle.

3. Calculation assumptions and evaluation criteria

3.1. Calculation assumptions

The simulations were carried out to the COOLCEP-S cycle by using the commercial Aspen Plus software [29], in which the component models are based on the energy balance and mass balance, with the default relative convergence error tolerance of 0.0001% which is used to determine whether a tear stream is converged or not, the tear stream is one for which Aspen Plus makes an initial guess, and iteratively updates the guess until two consecutive guesses are within a specified tolerance.

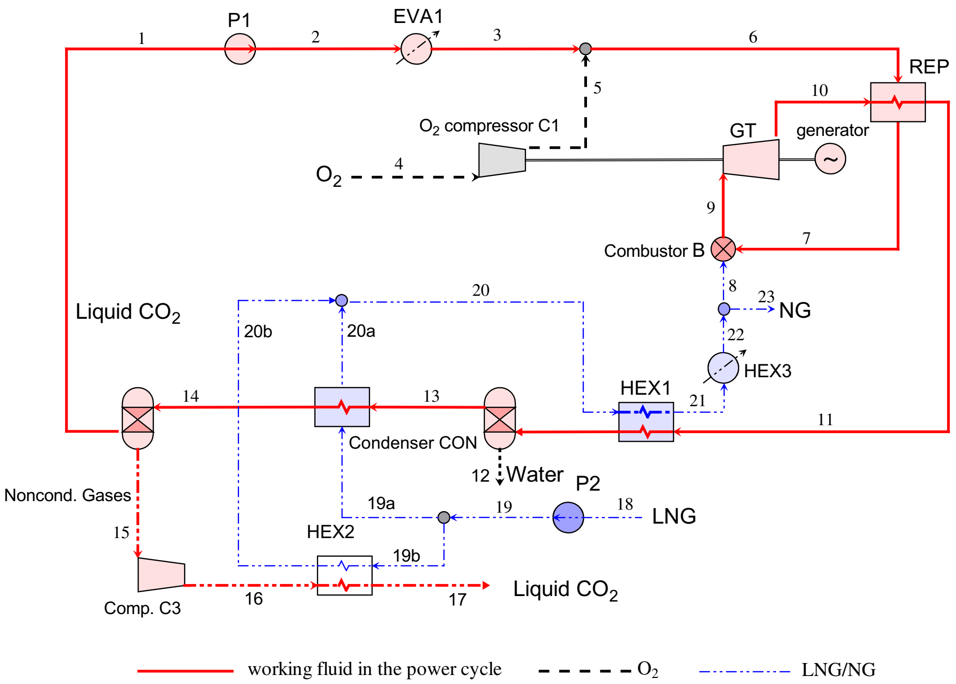

Fig. 1. The process flowsheet of the COOLCEP-S system.

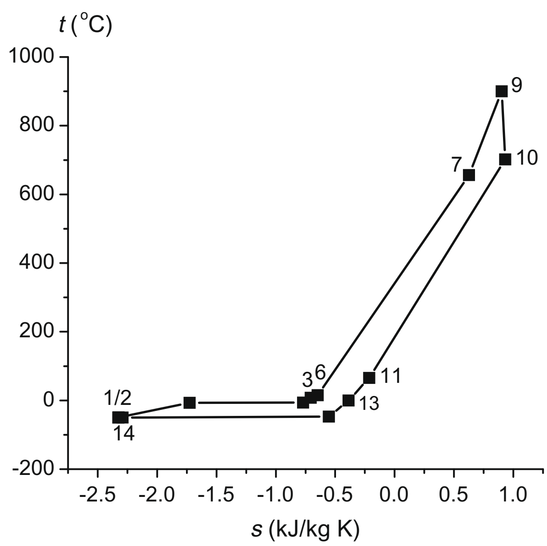

Fig. 2. Cycle *t*–*s* diagram in the COOLCEP-S system.

The tear stream is converged when the following is true for all tear convergence variables X including the total mole flow, all component mole flows, pressure, and enthalpy:

$$-tolerance < [(X_{calculated} - X_{assumed})/X_{assumed}] < tolerance$$

where the default for tolerance is 0.0001, $X_{assumed}$ is the assumed value of X before the calculation is conducted, $X_{calculated}$ is the calculated value of X.

The PSRK property method was selected for the thermal property calculations, which is based on the Predictive Soave–Redlich–Kwong equation of state model (an extension of the Redlich–Kwong–Soave equation of state). It can be used for mixtures of non-polar and polar compounds, in combination with light gases, and up to high temperatures and pressures. Some properties of feed streams are reported in Table 1, and the main assumptions for simulations are summarized in Table 2.

Table 1
Molar composition and some properties for feed streams.

	LNG	O_2
CH_4 (mol%)	90.82	
C_2H_6 (mol%)	4.97	
C_3H_8 (mol%)	2.93	
C_4H_{10}	1.01	
N_2 (mol%)	0.27	2
O_2 (mol%)		95
CO_2 (mol%)		
H_2O (mol%)		
Ar (mol%)		3
Temperature (°C)	−161.5	25
Pressure (bar)	1.013	2.38
Lower heating value (kJ/kg)	49,200	–
Power consumption for O_2 production (kJ/kg)		812

Oxygen (95 mol%) from a cryogenic ASU is chosen for the combustion, since this was considered to be the optimal oxygen purity when taking into account the tradeoff between the cost of producing the higher-purity oxygen and the cost of removing noncondensable species from the CO_2. The O_2 composition and its power consumption for production follow those in [26].

For the water separation, the turbine exhaust gas is cooled in HEX1 to 0 °C. Water is condensed and removed before CO_2 compression in C_2. To simplify the simulation it is assumed that water and CO_2 are fully separated.

3.2. Thermal performance evaluation criteria

The commonly used thermal power generation efficiency is defined as:

$$\eta_e = W_{net}/(m_f \cdot LHV) \quad (1)$$

Since the power and refrigeration cogeneration energy efficiency definition is problematic (cf. [30], for evaluating the cogeneration we use the exergy efficiency as:

$$\theta = (W_{net} + E_c)/(m_f \cdot e_f + m_{LNG} \cdot e_{LNG}) \quad (2)$$

Table 2
Main assumptions for the calculation of COOLCEP-S cycle.

Ambient state	
Temperature (°C)	25
Pressure (bar)	1.013
Combustor	
Combustor outlet temperature and pressure (°C/bar)	900/28
Pressure loss (%)	3
Efficiency (%)	100
Excess O_2 beyond the stoichiometric ratio (%)	2
Gas turbine	
Isentropic efficiency (%)	90
Turbine backpressure p_b (bar)	7.1
Gas turbine outlet temperature (°C)	700
Recuperator	
Pressure loss (%)	3
Minimal temperature difference (K)	45
LNG vaporization unit	
Pressure loss (%)	2–3
Temperature difference at pinch point (K)	8
CO_2 condenser	
Condensation pressure (bar)	7/60[a]
Condensation temperature (°C)	−50
Pump efficiency (%)	80
Compressor efficiency (%)	88
(Mechanical efficiency) × (generator electrical efficiency) (%)	96

[a] 7 bar is the condensation pressure for the main working fluid in the condenser; 60 bar is the condensation pressure for a small fraction of the working fluid in HEX2.

with both the power and cooling as the outputs, and both the fuel exergy and LNG cold exergy as the inputs. The cooling rate exergy E_C is the sum of the refrigeration exergy produced in the evaporators EVA1 and HEX3. In the calculation below, the processed LNG mass flow rate is chosen to be the least which can sustain the cooling demand of the power cycle exothermic process.

The CO_2 recovery ratio R_{CO_2} is defined as:

$$R_{CO_2} = m_{R,CO_2}/m_{COM,CO_2} \tag{3}$$

where m_{COM,CO_2} is the mass flow rate of the combustion-generated CO_2, and m_{R,CO_2} is the mass flow rate of the liquid CO_2 (17) that is retrieved.

To avoid CO_2 freezing, the condensation temperature in CON is chosen to be above −50 °C. The simulation has shown that at the condensation pressure of 7 bar, the mass flow rate of the condensed CO_2 is merely sufficient for the working fluid recycling; and that the condensed CO_2 flow rate increases as the condensation pressure increases. The higher condensation pressure, however, requires more compressor work, resulting in lower system efficiency. Considering the significant influence of the condensation pressure on both system thermal performance and the CO_2 recovery, the working fluid is compressed to 7 bar, and then the CO_2 is condensed for recycling as the working fluid. Only the remaining uncondensed working fluid that has a mass flow rate of only 2–5% of the total turbine exhaust after water removal, and high concentration of noncondensable species (the composition is about 88 mol% CO_2, and ~12 mol% of the noncondensable gases N_2, O_2 and Ar) will thus be compressed to a higher pressure for the CO_2 condensation and recovery.

3.3. Economic performance evaluation criteria

The preliminary economic analysis was based on the following assumptions:

- The cold energy of LNG is free, and we need not pay for it.
- The annual operation hours, H, is 7000 h/year, and the plant life, L_p, is 40 years.
- The annual interest rate is 8%.
- No loan is made for the total plant investment.

To optimize system configuration and design, we adopted and used four system economic performance criteria: (I) specific cost C_w, (II) cost of electricity *COE*, (III) system payback period *PY*, (IV) system net revenue R_{net}.

3.3.1. Specific cost C_w

The specific cost C_w is defined as the ratio between the total plant investment C_i and the cycle net power output W_{net}.

$$C_w = \frac{C_i}{W_{net}} \tag{4}$$

where the total plant investment, C_i, is the sum of the costs of all the hardware (dynamic equipments C_{DYN}, heat exchangers C_{HEX}, the conventional LNG evaporators C_{EVA}, and the balance of plant C_{BOP}). It should be pointed out that the conventional LNG evaporators is necessary as a backup for the LNG vaporization in case of the plant shutdown due to routine maintenance or emergency.

Balance of plant consists of the remaining systems, components, and structures that comprise a complete power plant or energy system that are not included in the prime mover [31]. As the systems are more complex than the conventional power generation system, here we assumed that the BOP accounts for 20% of the known component cost of the system.

3.3.2. Cost of electricity (COE)

The cost of electricity in the operation period is calculated as:

$$COE = \frac{\beta C_i + c_m + c_f - r_{CO_2} - \lambda \cdot r_{ref}}{H \cdot W_{net}} \tag{5}$$

c_m is the annual cost of operating and maintenance (O&M), assumed to be 4% of the total plant investment, C_i [32]. Taxes and insurance are not considered in this preliminary evaluation. c_f is the annual fuel cost, and r_{CO_2} is the annual CO_2 credit defined as the product of the annual CO_2 emission reduction multiplied by the CO_2 tax. H is the annual operation hours. β is a function of interest rate and the plant operation life n:

$$\beta = i/[1-(1+i)^{-n}] \tag{6}$$

with n = 40 and i = 8%, β = 0.08386. $\lambda \cdot r_{ref}$ is the actual annual refrigeration revenue because the refrigeration production may not be all sold out, so we adopt a refrigeration revenue factor λ with a range of 0–1 (0 for the case of no cooling requirement from users, 1 when all the refrigeration is sold) to indicate how much we can benefit from the refrigeration. The refrigeration price is assumed to be the same as the price of the electric power that would have been needed to supply the same cooling capacity Q_C by using state of the art vapor compression refrigeration machinery. The needed electricity, W_{comp} is thus calculated by

$$W_{comp} = Q_C/COP \tag{7}$$

where the *COP* (coefficient of performance) is assumed to be 7, a normal value for the compression refrigerating which normally can provide refrigeration with the temperature of 5 °C. It should be pointed out that, in practice, the refrigeration price is influenced by many other non-technical factors such as the market demands, climate change and artificial interference.

3.3.3. System payback period (PY)

The net current value, P, within n years is calculated as [33]:

$$P = B \cdot \left[\frac{(1+i)^n - 1}{i(1+i)^n}\right] \tag{8}$$

with n = 1, 2, ..., 40, and i = 8%, B is the annual value

$$B = r_{CO_2} + r_e + \lambda \cdot r_{ref} - C_f - C_m \tag{9}$$

r_e is the annual electricity power revenue defined as the product of the annual electricity output multiplied by the electricity price,

Table 3
Equipment and product cost information.

Equipment	Price	Equipment	Price (10^3 \$/m^2)
ASU	1376×10^3 \$/(kg O_2/s)	Recuperator	0.244
O_2 compressor C1	164.5×10^3 \$/(kg/s)	Condenser	0.097
Compressor C3	164.5×10^3 \$/(kg/s)	Heat exchangers	0.097
LNG pump P2	3.44×10^3 \$/(kg/s)	Evaporator EVA1	0.097
CO_2 pump P1	3.2×10^3 \$/(kg/s)		
Product	Price	Product	Price (\$/kW h)
Fuel	0.197 \$/N m^3	Electricity	0.059
CO_2 tax	0.033×10^3 \$/(ton CO_2)	Refrigeration	0.059

when the cash flow P is equal to the total plant investment C_i. The related value of n is the payback period PY.

3.3.4. Total net revenue (R_{net})

The system total net revenue, R_{net}, within the plant life L_p of 40 years is the sum of the total gross revenue R_g minus the total plant investment C_i.

$$R_{net} = R_g - C_i = L_p \cdot r_{net} - C_i \tag{10}$$

where r_{net} is the system annual net revenue,

$$r_{net} = r_{CO_2} + r_e + \lambda \cdot r_{ref} - c_f - c_m - \beta \cdot C_i \tag{11}$$

Table 3 presents the equipment and product information from the manufactures [34–37] and the product price in China, except the turbine price.

The price of the gas turbine, Y_{GT}, is calculated based on a costing correlation we developed (from data in the Gas Turbine World Handbook 2005–2006) for mechanical drive gas turbines,

$$Y = 76.07 - \frac{63.735 \times 10^3}{W_{GT}} + \frac{6.21 \times 10^6}{W_{GT}^2} - \frac{2.514 \times 10^8}{W_{GT}^3} + \frac{4.669 \times 10^9}{W_{GT}^4} - \frac{3.271 \times 10^{10}}{W_{GT}^5} + 1343.02\eta_e - 1635.07\eta_e^2 \tag{12}$$

where Y (\$/kW) is the cost; W_{GT} (MW) is the turbine power output; and η_e is the thermal efficiency.

It should be pointed out that Eq. (12) is intended for the price calculation of conventional simple gas turbines. To account for the fact that the turbine in our system uses CO_2 as the working fluid, which may require some modifications of conventional turbines, we multiplied by 1.5 the price calculated by Eq. (12), which is based on the price of the model UGT-15000 + 20 MW turbine[1] of 289 \$/kW (excluding compressor). As a result, the turbine price, Y_{GT}, is the product of the price Y obtained from Eq. (12) multiplied by the modification factor γ. Finally, Y_{GT} is of the form,

$$Y_{GT} = \gamma \cdot Y \tag{13}$$

4. Sensitivity analysis of the pinch point temperature differences in the major heat exchangers

In the COOLCEP-S cycle, lowering the temperature difference ΔT_p in the heat transfer processes is helpful to improve the cycle thermal performance, but at the same time requires larger and thus more expensive heat exchangers. Hence, a sensitivity analysis was carried here out of the COOLCEP-S cycle to study the effect of the pinch point temperature differences (ΔT_{p1} in the recuperator REP and ΔT_{p2} in the CO_2 condenser CON) on the cycle thermal performance and the economic performance.

[1] Zorya–Mashproekt State Enterprise Gas Turbine Research & Production Complex, Ukraine.

In the following calculation, the assumptions are kept unchanged as shown in Table 2, except the pinch point temperature differences, 45 K of ΔT_{p1} in recuperator and 8 K of ΔT_{p2} in CO_2 condenser.

4.1. Effect of the pinch point temperature difference ΔT_{p1} in the recuperator REP

4.1.1. Effect of ΔT_{p1} on the cycle thermal performance

With the same net power output W_{net} of 20 MW, simulation computation is made of the basic cycle for values of ΔT_{p1} from 45 K to 90 K. The heat exchanger transfer area estimation and the cycle thermal performance are shown in Tables 4 and 5. It should be pointed out that the heat transfer area estimation here is rough and based on the assumption that the heat exchangers are of the shell-and-tube type, and using average typical overall heat transfer coefficient values for these heat exchangers and fluids as found in the process heat transfer literature [38]. The recuperator REP is a conventional gas-to-gas heat exchanger; the heat exchanger HEX1 is also a gas-to-gas exchanger, HEX2 is a heat exchanger with phase change of gas-to-liquid in the hot side (16–17), and of LNG (containing some noncondensable gas) vaporizing in the cold side (19b–20b). The condenser CON consists of two parts, in the first part cooling of the CO_2 gas by the colder natural gas, followed by the second part in which CO_2 is then condensed due to cooling by liquid, boiling and gaseous natural gas, with an overall heat transfer coefficient of 600 W/m^2 K; the hot stream in EVA1 and HEX3 is assumed to be water with the inlet and outlet temperatures of 25 and 20 °C, respectively.

As shown in Table 4, as ΔT_{p1} is increased from 45 K to 90 K, the heat duty Q of the REP keeps decreasing and thus the heat transfer area A of the REP decrease too although they are always higher than those in the other heat exchangers. Fig. 3 explains the reason of the heat duty change in the REP: the hot side inlet temperature t_{10} is maintained fixed because of the fixed turbine inlet temperature t_9 and pressure ratio p_9/p_{10}, and the cold side inlet temperature t_6. The ΔT_{p1} always appears on the hot end of REP irrespective of its changes in this analysis. Hence, looking at Fig. 3, the t_7 decreases and the t_{11} increases. As a result, the ΔT_{p1} temperature changes lead to the heat duty changes in the REP despite the mass flow rate increase of the working fluid in it.

Table 4 indicates the heat transfer area A in REP is reduced by 52% (or, by 8047 m^2) as the ΔT_{p1} is increased from 45 K to 90 K; while the total heat transfer area of all heat exchangers in the system, ΣA, is reduced by 30% (7483 m^2), which is less than the decrease for REP alone because the increase of ΔT_{p1} causes some increase in the LNG evaporation unit area.

Table 5 indicates that the increase of ΔT_{p1} causes the increase of work input/output of the dynamic equipment (pumps P1 and P2, compressors C1 and C3, gas turbine GT). This is because the increase of ΔT_{p1} leads to the decrease of the inlet temperature of combustor B (t_7) as shown in Fig. 3, causing more fuel input to the combustor, and thus the working fluid flow rate going through

Table 4
Estimation of heat transfer areas, A, for different ΔT_{p1}.

ΔT_{p1} (K)	Unit		Q (MW)	LMTD (K)	U (W/m^2 K)	A (m^2)	A (%)	ΣA (m^2)
45 (Basic case)	Recuperator	REP	74.17	51.5	93	15,487	62.2	24,892
	LNG evaporation unit	CON	44.81	29.6	99/600	4159	16.7	
		HEX1	9.75	77.2	99	1275	5.1	
		HEX2	0.9	55.9	600	27	0.1	
	Evaporation unit	EVA1	42.42	33.6	429	2943	11.8	
		HEX3	14.51	33.8	429	1001	4	
60	Recuperator	REP	72.77	68.2	93	11,473	54.4	21,097
	LNG evaporation unit	CON	45.14	29.6	99/600	4205	19.9	
		HEX1	12.1	81.1	99	1507	7.1	
		HEX2	0.96	39.7	600	40	0.2	
	Evaporation unit	EVA1	42.68	33.6	429	2961	14	
		HEX3	12.27	31.4	429	911	4.3	
75	Recuperator	REP	71.37	84.7	93	9060	48	18876
	LNG evaporation unit	CON	45.49	29.3	99/600	4286	22.7	
		HEX1	14.49	85.1	99	1720	9.1	
		HEX2	1.02	77.6	600	22	0.1	
	Evaporation unit	EVA1	42.95	33.6	429	2980	15.8	
		HEX3	9.95	28.7	429	808	4.3	
90	Recuperator	REP	69.95	101.1	93	7440	42.7	17,409
	LNG evaporation unit	CON	45.83	29.3	99/600	4336	24.9	
		HEX1	16.9	89	99	1919	11	
		HEX2	1.08	71.4	600	25	0.1	
	Evaporation unit	EVA1	43.23	33.6	429	2999	17.2	
		HEX3	7.64	25.8	429	690	4	

Table 5
Cycle thermal performance for different ΔT_{p1}.

		ΔT_{p1} (K)			
		45 (Basic cycle)	60	75	90
Net power output, W_{net} (MW), kept constant		20	20	20	20
Heat duty (MW)	REP	74.17	72.77	71.37	69.95
	CON	44.81	45.14	45.49	45.83
	HEX1,2	10.65	13.06	15.51	17.98
Work (MW)	W_{loss}[a]	0.831	0.832	0.833	0.834
	W_{ASU}	2.338	2.493	2.654	2.817
	P1	0.269	0.271	0.272	0.274
	P2	1.906	1.918	1.93	1.942
	C1	0.924	0.985	1.049	1.114
	C3	0.264	0.282	0.3	0.318
	GT	26.533	26.781	27.038	27.299
Refrigeration					
EVA1	Temperature range (°C)	−49.4 to 8	−49.4 to 8	−49.4 to 8	−49.4 to 8
	Cooling capacity (MW)	42.42	42.68	42.95	43.23
	Exergy (MW)	6.57	6.61	6.66	6.67
HEX3	Temperature range (°C)	−34.7 to 8	−29.3 to 8	−23.1 to 8	−16.4 to 8
	Cooling capacity (MW)	14.51	12.27	9.95	7.64
	Exergy (MW)	2.387	1.844	1.363	0.95
	Total cooling capacity, Q_C (MW)	56.94	54.95	52.90	50.87
	Total exergy, E_C (MW)	8.96	8.46	8.02	7.65
Mass flow rate (kg/s)	Main working fluid, m_{wf}	101.61	102.23	102.88	103.54
	Retrieved liquid CO_2, $m_{co2,rec}$	1.846	1.971	2.098	2.228
	NG fuel, m_{fuel}	0.688	0.735	0.783	0.831
	LNG, m_{LNG}	95.54	96.122	96.735	97.356
Thermal efficiency, η_e (%)		59.1	55.3	51.9	48.9
Exergy efficiency, θ (%)		39.8	37.7	36.0	34.2

[a] Work loss associated with the mechanical efficiency and generator electrical efficiency.

the dynamic equipments increases (while the pressure changes across them remain the same).

We then examine the refrigeration output from the evaporators EVA1 where the low temperature liquid CO_2 is evaporated, and from HEX3 where the low temperature NG is heated to the near environment temperature. As the ΔT_{p1} is increased, Table 5 shows that the cooling capacity and refrigeration exergy in the evaporator EVA1 increase, and that is entirely because of the associated increase in the liquid CO_2 mass flow rate, since the refrigeration temperature range is maintained fixed. Things are different in the HEX3: as the ΔT_{p1} increases, both the HEX3 inlet temperature t_{21} and the LNG flow rate increase, and these two factors have opposite effects on the refrigeration output. The calculation results indicate that the negative effect of the former one dominates so overall that the refrigeration production in HEX3 decreases. It can be seen from Table 5 that the reduction of refrigeration output in HEX3 surpasses the increment in EVA1, so there are reductions of 10.7% (6.1 MW) in the total cooling

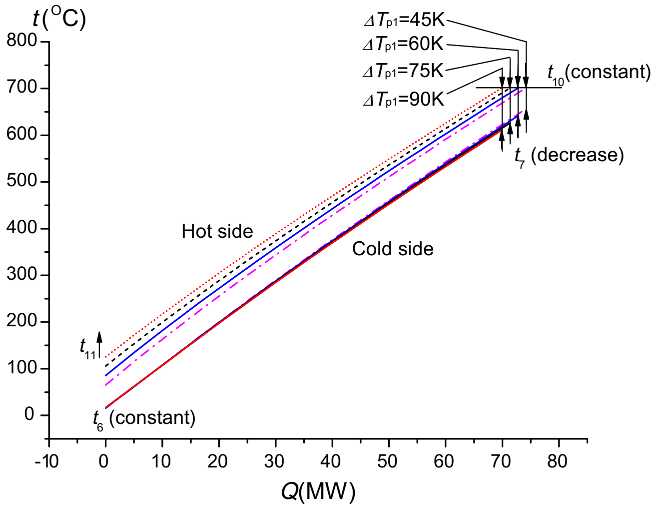

Fig. 3. t–Q diagram in REP for different ΔT_{p1}.

capacity Q_C, and of 14.6% (1.3 MW) in the total refrigeration exergy output E_C.

Fig. 4 shows that the increase of ΔT_{p1} is unfavorable for the cycle efficiencies. As ΔT_{p1} is increased from 45 K to 90 K, the thermal efficiency η_e declines from 59.1% to 48.9%, a reduction of 17.3%; and the exergy efficiency θ declines from 39.8% to 34.2%, a reduction of 14.1%.

4.1.2. Effect of ΔT_{p1} on the cycle economic performance

Based on the cycle thermal performance results shown in Table 5, an economic analysis of the effect of ΔT_{p1} on cycle economic performance, including the system specific cost C_w, cost of electricity *COE*, payback period *PY*, total net revenue R_{net}, etc., is performed and the results are summarized in Table 6 with the assumption of 40 years of plant life L_p, 7000 of annual operation hours H and 20 MW of net cycle power output W_{net}.

The results of the economic analysis are shown in Table 6 and Figs. 5–9, and the following conclusions are drawn:

Increasing ΔT_{p1} from 45 K to 90 K indeed results in a reduction of 40.7% (1,907,000 $) in the cost of heat exchangers C_{HEX}

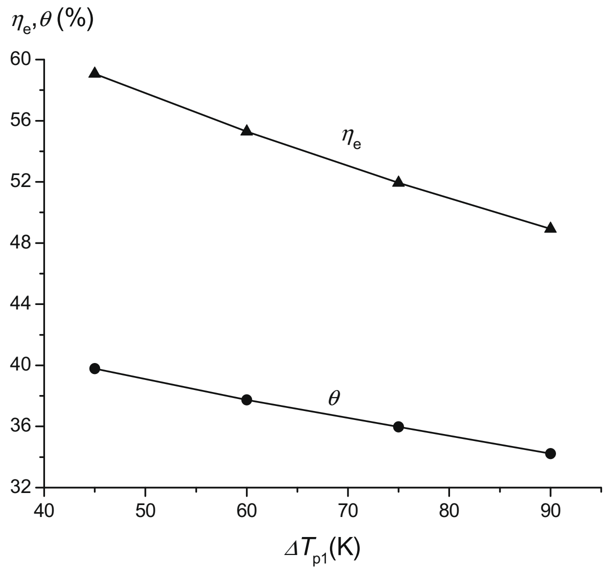

Fig. 4. Effect of ΔT_{p1} on the thermal efficiency η_e and exergy efficiency θ.

mainly due to the decrease in the heat transfer areas, but also results in a counterproductive increase of 22.3% (2,865,000 $) in the cost C_{DYN} of the dynamic equipment among which the increase of gas turbine cost is caused by the increase of W_{GT} and the decrease of η_e (see Eqs. (12) and (13)) and the increase of the other equipment's cost is caused by the increase of working fluid flow rate. Overall, that increase of ΔT_{p1} causes a 5.4% increase (1,159,000 $) in the total plant investment C_i, and thus the related O&M cost increases by 47,000 $/year. Increasing ΔT_{p1} also increases the annual fuel cost by 21% (888,000 $/year).

The system revenue is composed of three parts: (i) the CO_2 credit r_{CO_2} that is the revenue due to the reduction of CO_2 emission; one of the most important characteristics of this cycle is zero-CO_2-emission which enables the power plant to benefit from CO_2 emission allowance trading. Since more fuel is consumed as ΔT_{p1} increases from 45 K to 90 K, more CO_2 is produced and retrieved, therefore, the related revenue also increases by 20.7%, 318,000 $/year; (ii) the electricity revenue r_e remains unchanged because the net power output is assumed to be fixed as 20 MW for all values of ΔT_{p1} increases, but here we prefer to use the net electricity revenue r_{ne} which is defined as the electricity revenue r_e reduced by the fuel cost c_f, which in total shows a reduction of 22%, 888,000 $/year totally due to the increment of the fuel cost; (iii) the actual refrigeration revenue $\lambda \cdot r_{ref}$ depends on the refrigeration market availability extent expressed by λ that can assume any value between 0 and 1. Table 6 shows that the upper limit ($\lambda = 1$) of refrigeration revenue r_{ref} is reduced by 10.7%, 358,000 $/year.

Based on the above analysis of cycle cost and revenue, the increase of ΔT_{p1} from 45 K to 90 K affects the specific cost C_w, total net revenue R_{net}, cost of electricity *COE* and payback period *PY* as follows:

(1) Specific cost C_w increases. According to Eq. (4) and Table 6, the 5.4% increase (1,159,000 $) in the total plant investment C_i leads to and a 5.4% increase of C_w from 1075 $/kW to 1133 $/kW.
Since the actual refrigeration revenue $\lambda \cdot r_{ref}$ varies with the value of the refrigeration revenue factor λ, we consider the total net revenue R_{net}, the cost of electricity *COE* and the payback period *PY*, respectively, as a function of the refrigeration revenue factor λ as well as of the pinch point temperature difference ΔT_{p1}. So the following analysis will discuss not only the effects of ΔT_{p1} and but also the effects in two extreme cases of $\lambda = 0$ and $\lambda = 1$.
(2) Cost of electricity *COE* increases. According to Eqs. (5)–(7) and Table 6, as ΔT_{p1} increases from 45 K to 90 K: (i) for $\lambda = 0$, the resulting increase of the sum of all the cost $(\beta \cdot C_i + c_m + c_f)$ surpasses the increase of the CO_2 credit r_{CO_2}, and the cost of electricity *COE* thus increases by 13.4%; (ii) for $\lambda = 1$, the refrigeration revenue r_{ref} decreases with the increase of ΔT_{p1}, causing that the reduction of $(r_{CO_2} + r_{ref})$ surpasses the increase of $(\beta \cdot C_i + c_m + c_f)$, and the cost of electricity *COE* thus increases by 53.1%.
(3) System payback period *PY* is prolonged. Table 6 indicates that the annual value B decreases and the total plant investment C_i increases, and therefore (Eq. (8)): (i) for $\lambda = 0$, the system payback period *PY* increases from 5.91 years to 7.61 years and (ii) for $\lambda = 1$, the *PY* increases from 3.12 years to 3.84 years.
(4) Total net revenue R_{net} decreases. According to Eq. (10) for R_{net}, the reduction of the net annual revenue r_{net} and increase of the total plant investment C_i in a reduction of 31.4% (29,719,000 $/40 years) for $\lambda = 0$, and 19.2% (44,039,000 $/40 years) for $\lambda = 1$.

Table 6
Economic estimation for different ΔT_{p1}.

	ΔT_{p1} (K)			
	45 (Base case)	60	75	90
Operation time of plant (h year^{-1})	7000			
Cost of dynamic equipments C_{DYN} (10^3 $)				
GT	7680	8517	9122	9552
ASU	3956	4226	4497	4775
C1, C3, P1, P2	1201.8	1259.2	1317.6	1376
Total	12,838	14,002	14,937	15,703
Cost of heat exchangers, C_{HEX} (10^3 $)				
REP	3778	2799	2211	1815
CON	403	408	416	421
HEX1,2	126	150	169	189
EVA1, HEX3	383	376	367	358
Total (10^3 $)	4690	3733	3163	2783
Cost of conventional LNG evaporators, C_{EVA} (10^3 $)	395	398	400	403
BOP, C_{BOP} (20%) (10^3 $)	3585	3627	3700	3778
Total plant investment, C_i (10^3 $)	21,508	21,760	22,200	22,667
Specific cost, C_w ($/kW)	1075	1088	1110	1133
Cost of O&M, c_m (10^3 $/year)	860	870	888	907
Fuel cost, c_f (10^3 $/year)	4225	4523	4820	5113
Revenue				
Electricity revenue, r_e (10^3 $/year)	8260	8260	8260	8260
Net electricity revenue, r_{ne} [a] (10^3 $/year)	4035	3737	3440	3147
CO_2 credit, r_{CO2} (10^3 $/year)	1535	1639	1745	1853
Refrigeration revenue, r_{ref} (10^3 $/year)	3359	3242	3122	3001
Net annual revenue, r_{net} (10^3 $/year)				
($\lambda = 0$)	2906	2681	2435	2192
($\lambda = 1$)	6265	5923	5557	5193
Total net revenue, R_{net} (10^3 $/40 yrs)				
($\lambda = 0$)	94,732	85,480	75,200	65,013
($\lambda = 1$)	229,092	215,160	200,080	185,053
COE ($/kWh)				
($\lambda = 0$)	0.0382	0.04	0.0416	0.0433
($\lambda = 1$)	0.0143	0.0167	0.0193	0.0219
Payback years (with plant lilfe of 40 years)				
($\lambda = 0$)	5.91	6.35	6.93	7.61
($\lambda = 1$)	3.12	3.31	3.56	3.84

[a] The net electricity revenue, r_{ne}, is defined as the sum of the electricity revenue r_e minus the fuel cost c_f.

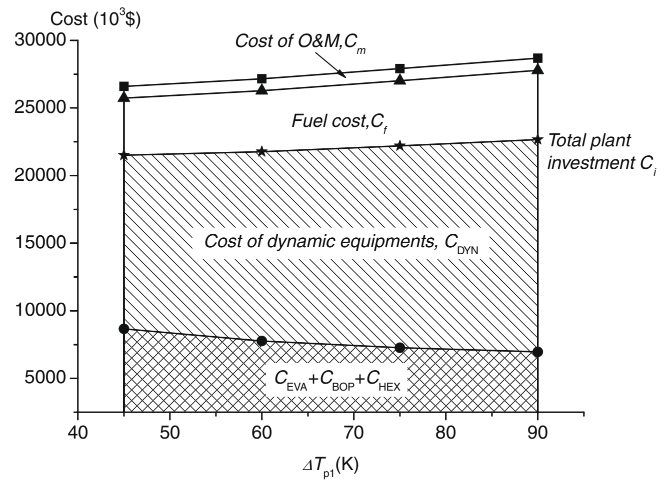

Fig. 5. Effect of ΔT_{p1} on cycle costs.

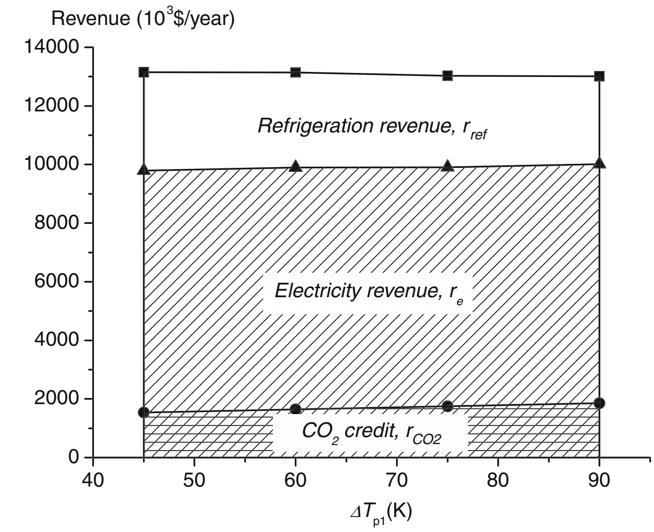

Fig. 6. Effect of ΔT_{p1} on cycle revenues.

It is thus concluded that the increase of the ΔT_{p1} from 45 K to 90 K has negative effects on the cycle economic performance and makes it obvious that the optimal design in the considered range of parameters is at the lowest practical ΔT_{p1} = 45 K originally assumed in the system development.

It was also found that, for the same ΔT_{p1}, the system has a much better economic performance for $\lambda = 1$ than for $\lambda = 0$: the total net revenue R_{net} is 142% higher, *COE* is 50% lower, and *PY* is shortened by at least 2.8 years.

4.2. Effect of the pinch point temperature difference ΔT_{p2} in the CO_2 condenser CON

Among the needed heat exchangers, second to the size of the recuperator REP is the CO_2 condenser CON. In the following section, a sensitivity analysis is made of the thermal and economic effect of the pinch point temperature difference ΔT_{p2} in CON. ΔT_{p1} in REP is fixed at its near-optimal value of 45 K, and other main assumptions, including the turbine inlet/outlet parameters and the CO_2 condensation pressure/temperature are maintain unchanging as in the basic cycle where the values were fixed at ΔT_{p1} = 45 K, ΔT_{p2} = 8 K.

4.2.1. Effect of ΔT_{p2} on the cycle thermal performance

With the same net power output W_{net} of 20 MW, simulation calculations are made to the basic cycle as the ΔT_{p2} is varied from 8 K (the practical minimum, used in the basic cycle) to 17 K. Tables 7 and 8 show the heat exchanger transfer area estimation and the cycle thermal performance under different ΔT_{p2}, respectively.

Fig. 10 is the t–Q diagram of CON, it can be seen that the heat duty of CON rises by 1.8% (0.82 MW) as the ΔT_{p2} is raised from 8 K to 17 K. As assumed in the basic case, all the inlet and outlet temperatures (t_{13}, t_{14} and t_{19a}) of CON, except the cold side outlet temperature t_{20a}, are maintained fixed as the ΔT_{p2} is increased, so the increase of ΔT_{p2} is accomplished only by the decrease of t_{20a}. This moves the hot side stream temperature curve to the right, and the mass flow rate of the working fluid and the LNG through the CON increase as well, therefore the heat duty of CON increases.

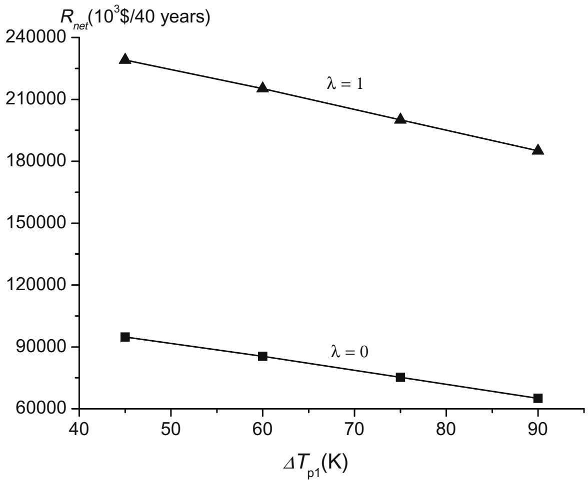

Fig. 7. Effect of ΔT_{p1} on total net revenue R_{net}.

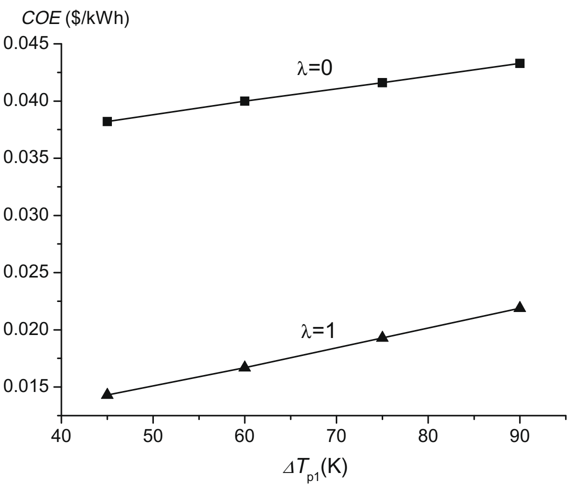

Fig. 8. Effect of ΔT_{p1} on the cost of electricity COE.

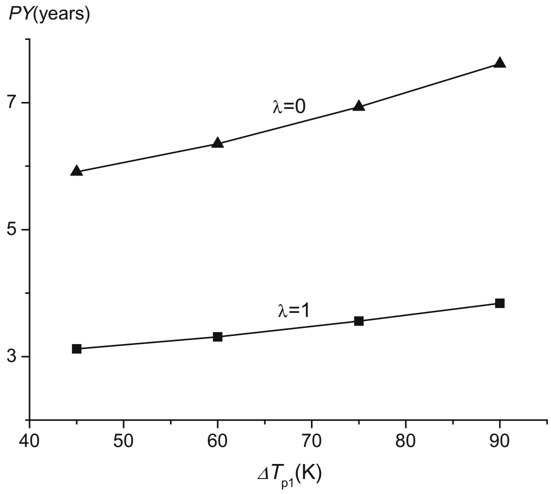

Fig. 9. Effect of ΔT_{p1} on payback period PY.

At the same time, the mass flow rate of the working fluid and the LNG through the other heat exchangers will increase as well, leading to the increase of heat duties in all the heat exchangers as shown in Table 7.

Although the heat duties of all the heat exchangers rise with the increase of ΔT_{p2}, the heat transfer areas vary in completely different ways. As shown in Table 7, the heat transfer areas of heat exchangers REP and EVA1 (in the power subcycle) rise as ΔT_{p2} increases, because their LMTD-s remain unchanged while their heat duties increase. For the heat exchangers CON, HEX1,2 and HEX3, their heat transfer areas decrease as ΔT_{p2} increases because their LMTD-s and heat duties increase but the LMTD-s increase more than the heat duties. The heat transfer area decrease in the LNG evaporation unit dominates over the area increase in the power subcycle, with a subsequent overall reduction of 2% (~500 m^2) in the total area ΣA as ΔT_{p2} is increased from 8 K to 17 K.

Fig. 11 illustrates the effect of ΔT_{p2} on the thermal efficiency η_e and exergy efficiency θ. As the ΔT_{p2} increases from 8 K to 17 K, the working fluid mass flow rate increases and the cycle specific power decreases. As a result, the net power output remains the same (20 MW), at the same time 1.9% (0.6 MW) more fuel energy input is required in the combustor B, and therefore the η_e drops by 1.8%. Also, more LNG flows through the cycle and thus 22% (8.2 MW) more LNG exergy is consumed and 43% (3.9 MW) more refrigeration exergy is produced, so the sum of exergy outputs is increased by 13.4% and the sum of exergy inputs is increased by 12%. As a result, the exergy efficiency θ has a 1.2% increase.

4.2.2. Effect of ΔT_{p2} on the cycle economic performance

Based on the simulation results shown in Tables 7 and 8, an analysis of the economic effect of ΔT_{p2} was performed and the cycle economic performance for different ΔT_{p2} is summarized in Table 9. The main assumptions are plant life L_p = 40 years, annual operation H = 7000 h, and net cycle power output W_{net} = 20 MW.

Table 9 and Figs. 12–16 indicate the economic effects of increasing ΔT_{p2} from 8 K to 17 K, as follows:

As shown in Fig. 12 and Table 9, there is little effect on the cost of heat exchangers C_{HEX}, but it results in an increase of 3.7% (476,000 $) in the cost C_{DYN} of the dynamic equipment because of the increase of the working fluid flow rate. Overall, that increase of ΔT_{p2} causes a 3.1% increase (667,000 $) in the total plant investment C_i, and thus the related O&M cost increases by 27,000 $/year. Increasing ΔT_{p2} also causes the annual fuel cost to increase by 1.9% (79,000 $/year).

Table 7
Estimation of heat transfer area, A, for different ΔT_{p2}.

ΔT_{p2} (K)	Unit		Q (MW)	LMTD (K)	U (W/m^2 K)	A (m^2)	A (%)	ΣA (m^2)	Q (MW)
8 (Base case)	Power subcycle	REP	74.17	51.5	93	15,487	18,430	62.2	24,892
		EVA1	42.42	33.6	429	2943		11.8	
	LNG evaporation unit	CON	44.81	29.6	99/600	4159	6462	16.7	
		HEX1	9.75	77.2	99	1275		5.1	
		HEX2	0.9	55.9	600	27		0.1	
		HEX3	14.51	33.8	429	1001		4	
11	Power subcycle	REP	74.58	51.5	93	15,572	18,531	63.4	24,555
		EVA1	42.66	33.6	429	2959		12.1	
	LNG evaporation unit	CON	45.06	34.3	99/600	3588	6024	14.6	
		HEX1	9.8	81.4	99	1216		4.9	
		HEX2	0.9	66.7	600	23		0.1	
		HEX3	18.94	36.9	429	1197		4.9	
14	Power subcycle	REP	75.04	51.5	93	15,668	18,646	64.2	24,414
		EVA1	42.92	33.6	429	2978		12.2	
	LNG evaporation unit	CON	45.34	38.9	99/600	3175	5768	13	
		HEX1	9.86	84.8	99	1174		4.8	
		HEX2	0.91	74.8	600	20		0.1	
		HEX3	23.76	39.6	429	1399		5.7	
17	Power subcycle	REP	75.51	51.5	93	15,765	18,761	64.6	24,397
		EVA1	43.19	33.6	429	2996		12.3	
	LNG evaporation unit	CON	45.63	42.9	99/600	2879	5636	11.8	
		HEX1	9.92	87.8	99	1141		4.7	
		HEX2	0.91	80.8	600	19		0.1	
		HEX3	28.7	41.9	429	1597		6.5	

Table 8
Cycle thermal performance for different ΔT_{p2}.

		ΔT_{p2} (K)			
		8 (Base case)	11	14	17
Net power output, W_{net} (MW)		20	20	20	20
Heat duty (MW)	REP	74.17	74.58	75.04	75.51
	CON	44.81	45.06	45.34	45.63
	HEX1,2	10.65	10.7	10.77	10.83
Work (MW)	$W_{loss}{}^*$	0.831	0.833	0.834	0.835
	W_{ASU}	2.338	2.347	2.362	2.376
	P1	0.269	0.27	0.272	0.273
	P2	1.906	2.035	2.176	2.318
	C1	0.924	0.928	0.933	0.939
	C3	0.264	0.265	0.267	0.269
	GT	26.533	26.678	26.843	27.01
Refrigeration					
EVA1	Temperature range (°C)	−49.4 to +8	−49.4 to +8	−49.4 to +8	−49.4to +8
	Cooling capacity (MW)	42.42	42.66	42.92	43.19
	Exergy (MW)	6.57	6.61	6.65	6.69
HEX3	Temperature range (°C)	−34.7 to +8	−40.8 to +8	−45.8 to +8	−49.6to +8
	Cooling capacity (MW)	14.51	18.94	23.76	28.7
	Exergy (MW)	2.39	3.47	4.76	6.15
	Total cooling capacity Q_C (MW)	56.94	61.6	66.68	71.89
	Total exergy E_C (MW)	8.96	10.08	11.41	12.84
Mass flow rate (kg/s)	Main working fluid, m_{wf}	101.61	102.17	102.8	103.43
	Retrieved liquid CO_2, $m_{co2,rec}$	1.846	1.856	1.867	1.879
	NG fuel, m_{fuel}	0.688	0.692	0.696	0.701
	LNG, m_{LNG}	95.54	102	109.07	116.2
Thermal efficiency, η_e (%)		59.06	58.73	58.37	58.01
Exergy efficiency, θ (%)		39.79	39.82	39.99	40.25

Fig. 13 and Table 9 show the cycle revenue, which is composed of three parts: (i) the CO_2 credit r_{CO_2}; since more fuel is consumed as ΔT_{p2} increases, more CO_2 is produced and retrieved, therefore, the related revenue also increases by 1.8%, or 28,000 \$/year; (ii) the electricity revenue r_e remains unchanged because of the fixed net power output, but the net electricity revenue r_e drops by 2%, or 79,000 \$/year, entirely due to the increase of the fuel cost. Apparently, the reduction in the electric power revenue is much higher than the revenue increase due to zero-CO_2 emission; and (iii) the refrigeration revenue $\lambda \cdot r_{ref}$; the upper limit ($\lambda = 1$) of refrigeration revenue r_{ref} increases by 26.3%, 883,000 \$/year, mainly because an increase of 98%, 14.2 MW, in the refrigeration cooling capacity in the HEX3 caused by the increase of the LNG mass flow rate from 95.5 kg/s to 116.2 kg/s and the drop of the inlet temperature t_{21} from −35 °C to −50 °C.

Consequently, the effects of increasing ΔT_{p2} from 8 K to 17 K on the specific cost C_w, the total net revenue R_{net}, the cost of electricity COE and the payback period PY is as follows:

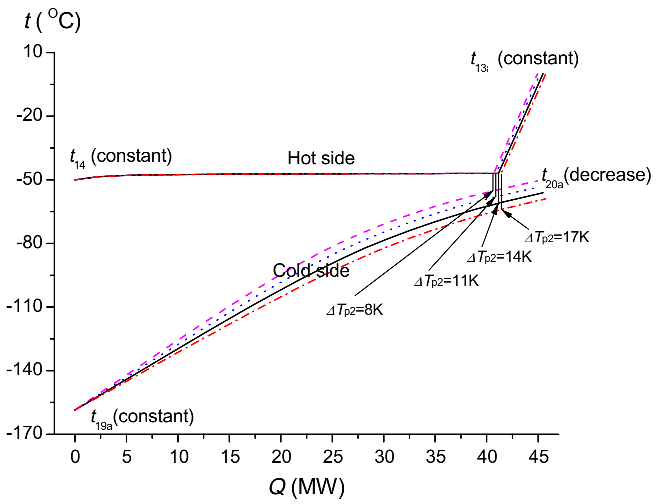

Fig. 10. t–Q diagram of the condenser CON under different ΔT_{p2}.

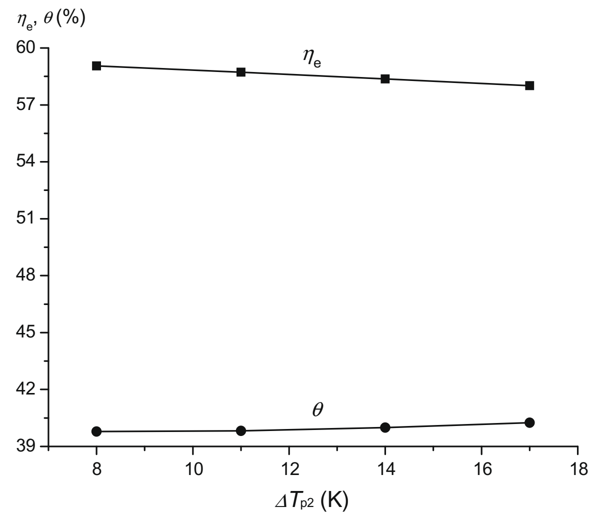

Fig. 11. Effect of ΔT_{p2} on the thermal efficiency η_e and exergy efficiency θ.

(1) The specific cost C_w increases: According to Eq. (4) and Table 9, the 3.1% increase (667,000 $) in the total plant investment C_i results in a 3.2% increase of C_w, from 1075 $/kW to 1109 $/kW.
Again, the effects are considered for the limiting cases $\lambda = 0$ and $\lambda = 1$ in the following analysis.

(2) Cost of electricity *COE*: According to the Eqs. (5)–(7) and Table 9, as ΔT_{p2} is increased from 8 K to 17 K: (i) for $\lambda = 0$, the resulting increase of the sum of all the cost $(\beta \cdot C_i + C_m + C_f)$ surpasses the increase of the CO_2 credit r_{CO_2}, and the cost of electricity *COE* thus increases by 2.6%

Table 9
Costing estimation for different ΔT_{p2}.

	ΔT_{p2} (K)			
	8 (Base case)	11	14	17
Operation time of plant (h year^{-1})	7000			
Cost of dynamic equipments, C_{DYN} (10^3 $)				
GT	7680	7777	7883	7998
ASU	3956	3978	4003	4028
C1, C3, P1, P2	1201.8	1229	1258.5	1287.8
Total (10^3 $)	12,838	12,984	13,145	13,314
Cost of heat exchangers, C_{HEX} (10^3 $)				
REP	3778	3800	3823	3847
EVA1	285	287	289	291
CON	403	348	308	279
HEX1,2	126	120	116	113
HEX3	98	116	136	155
Total (10^3 $)	4690	4671	4672	4685
Cost of the conventional LNG evaporators C_{EVA} (10^3 $)	395	422	451	480
BOP, C_{BOP} (10^3 $)	3585	3615	3654	3696
Total plant investment, C_i (10^3 $)	21,508	21,692	21,922	22,175
Specific cost, C_w ($/kW)	1075	1085	1096	1109
Cost of O&M, c_m (10^3 $/year)	860	868	877	887
Fuel cost, c_f (10^3 $/year)	4225	4250	4274	4304
Revenue				
Electricity revenue, r_e (10^3 $/year)	8260	8260	8260	8260
Net electricity revenue, r_{ne}[a] (10^3 $/year)	4035	4010	3986	3956
CO_2 credit, r_{CO2} (10^3 $/year)	1535	1544	1553	1563
Refrigeration revenue, r_{ref} (10^3 $/year)	3359	3634	3932	4242
Net annual revenue, r_{net} (10^3 $/year)				
($\lambda = 0$)	2906	2867	2824	2772
($\lambda = 1$)	6265	6501	6756	7014
Total net revenue, R_{net} (10^3 $/40 yrs)				
($\lambda = 0$)	94,732	92,984	91,023	88,721
($\lambda = 1$)	229,092	238,344	248,302	258,401
COE ($/kWh)				
($\lambda = 0$)	0.0382	0.0385	0.0388	0.0392
($\lambda = 1$)	0.0143	0.0126	0.0108	0.0089
Payback years, *PY* (with plant life of 40 years)				
($\lambda = 0$)	5.91	6.01	6.14	6.28
($\lambda = 1$)	3.12	3.06	2.97	2.9

[a] The net electricity revenue, r_{ne}, is defined as the sum of the electricity revenue r_e minus the fuel cost c_f.

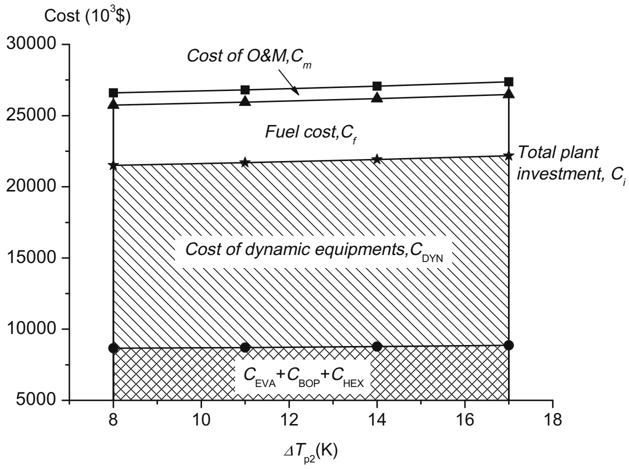

Fig. 12. Effect of ΔT_{p2} on cycle costs.

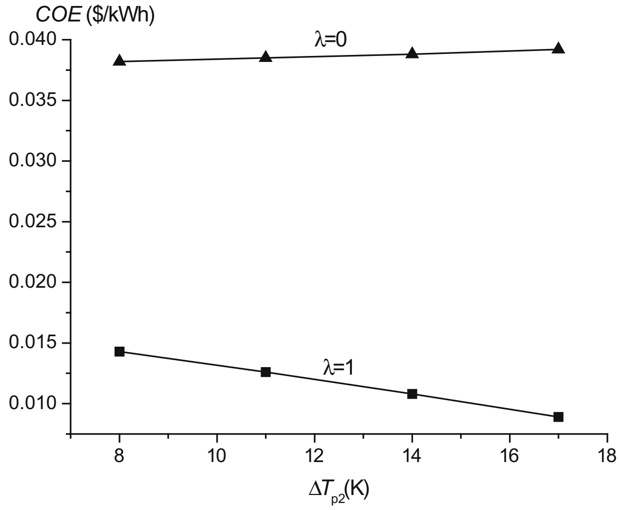

Fig. 15. Effect of ΔT_{p2} on the cost of electricity *COE.*

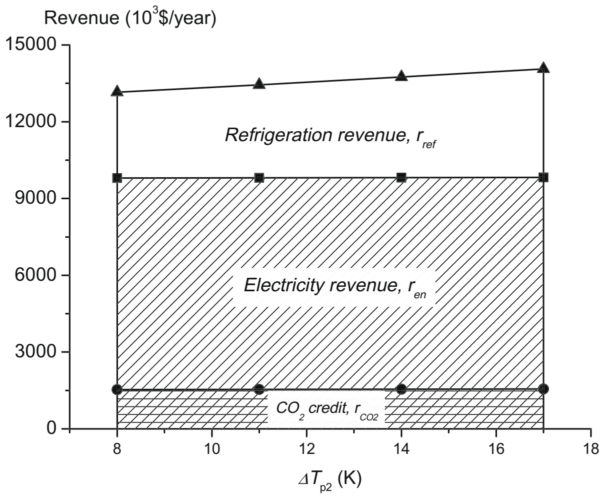

Fig. 13. Effect of ΔT_{p2} on cycle revenues.

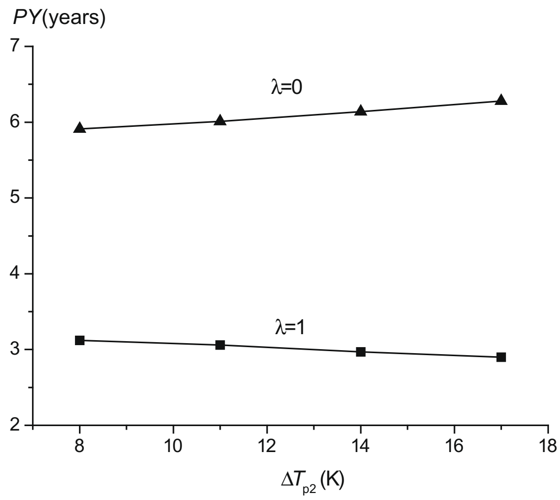

Fig. 16. Effect of ΔT_{p2} on the payback period *PY.*

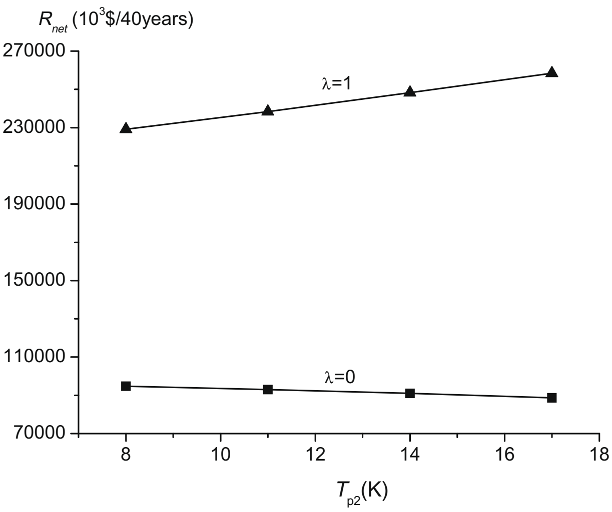

Fig. 14. Effect of ΔT_{p2} on total net revenue R_{net}.

and (ii) for $\lambda = 1$, it results in a 26.3% (883,000 \$/year) increase in the refrigeration revenue r_{ref} that is the main reason for a 37.8% reduction in the cost of electricity *COE*.

(3) System payback period *PY*: Table 9 shows that: (i) for $\lambda = 0$, the net annual revenue r_{net} decreases, thus prolonging the system payback period *PY* from 5.91 years to 6.28 years according to Eq. (8); (ii) for $\lambda = 1$, *PY* is shortened from 3.12 years to 2.9 years, mainly because of the increase in the annual value *B* caused by the increase in the refrigeration revenue r_{ref}.

(4) Total net revenue R_{net}: As ΔT_{p2} is increased from 8 K to 17 K: (i) for $\lambda = 0$, the reduction of the net annual revenue r_{net} and increase of the total plant investment C_i cause a 6.3% (6,011,000 \$/40 yrs) reduction in the total net revenue R_{net} according to Eq. (10) and (ii) for $\lambda = 1$, R_{net} increases by 12.8% (29,309,000 \$/40 yrs).

It is interesting to note from the above that increasing the ΔT_{p2} from 8 K to 17 K is unfavorable as evaluated by *COE*, *PY* and R_{net} for $\lambda = 0$, while it is favorable for $\lambda = 1$.

It was predicted, as shown in Figs. 14–16 that, at the same ΔT_{p2} the system economic performance is much better for $\lambda = 1$ than for

$\lambda = 0$: by a total net revenue R_{net} increase over 142%, over 62% decrease in the cost of electricity *COE*, and at least a 2.8 years shorter payback period *PY*.

5. Conclusions

A thermoeconomic analysis was performed aimed at optimization of a novel power and refrigeration cogeneration system, COOLCEP-S, which produces near-zero-CO_2 and other emissions and has high efficiency. To achieve these desirable attributes, it uses the liquefied natural gas (LNG) coldness during its revaporization. In that, we focus on the study of the thermodynamic and economic effect of the pinch point temperature differences of the two most important heat exchangers, ΔT_{p1} of the recuperator REP, and ΔT_{p2} of the CO_2 condenser CON in the COOLSEP-S system.

For the turbine inlet temperature of 900 °C and pressure ratio of 4, cycle net power output of 20 MW, plant life of 40 years and 7000 annual operation hours, and two extreme cases of refrigeration revenue: $\lambda = 0$ when this system has no financial benefit from the available refrigeration capacity and $\lambda = 1$ when all the refrigeration produced in this plant can be sold for revenue.

The increase of ΔT_{p1} from 45 K to 90 K causes the following changes:

(1) The cycle thermal performance is worsened by a reduction of 17% in the thermal efficiency η_e, and 14% in the exergy efficiency θ.
(2) The cycle economic performance is worsened too: the specific cost C_w increases by 5.4%, the cost of electricity *COE* increases by 13.4% ($\lambda = 0$) and by 53.1% ($\lambda = 1$), the system payback period *PY* is prolonged by ~1.7 years ($\lambda = 0$) and ~0.7 year ($\lambda = 1$), the total net revenue R_{net} is reduced by 31.4% ($\lambda = 0$) and by 19.2% ($\lambda = 1$).

The increase of ΔT_{p2} from 8 K to 17 K causes the following changes:

(1) The thermal efficiency η_e is reduced by a 1.8% and the exergy efficiency θ is increased by 1.2%.
(2) The specific cost C_w increases by 3.2%.
(3) For $\lambda = 0$, the cycle economic performance is worsened: the cost of electricity *COE* increases by 2.6%, the system payback period *PY* is prolonged by 0.37 year, and the total net revenue R_{net} is reduced by 6.3%.
(4) For $\lambda = 1$, the cycle economic performance is improved: the cost of electricity *COE* decreases by 37.8%, the system payback period *PY* is shortened by 0.22 years, and the total net revenue R_{net} increases by 12.8%.

The resulting main recommendations are: (1) the optimal design in the considered range of parameters is at the lowest practical $\Delta T_{p1} = 45$ K, (2) increasing ΔT_{p2} is unfavorable for *COE*, *PY* and R_{net} for $\lambda = 0$, but favorable for $\lambda = 1$, (3) for the same ΔT_{p1} or ΔT_{p2}, the system has a much better economic performance for $\lambda = 1$ than for $\lambda = 0$, (4) the cost of electricity in the base case ($\Delta T_{p1} = 45$ K, $\Delta T_{p2} = 8$ K) of this system is 0.0382 $/kWh (~0.3 CNY/kWh) and the payback period is 5.9 years, much lower than those of conventional coal power plants being installed at this time in China, and yet COOLSEP-S has the additional major advantage in that it produces no CO_2 emissions.

Acknowledgements

The authors gratefully acknowledge the support from the Statoil ASA, and the Chinese Natural Science Foundation Project (No. 50520140517).

References

[1] Karashima N, Akutsu T. Development of LNG cryogenic power generation plant. In: Proceedings of 17th IECEC; 1982. p. 399–404.
[2] Angelino G. The use of liquid natural gas as heat sink for power cycles. ASME J Eng Power 1978;100:169–77.
[3] Kim CW, Chang SD, Ro ST. Analysis of the power cycle utilizing the cold energy of LNG. Int J Energy Res 1995;19:741–9.
[4] Najjar YSH, Zaamout MS. Cryogenic power conversion with regasification of LNG in a gas turbine plant. Energy Convers Manage 1993;34:273–80.
[5] Wong W. LNG power recovery, proceedings of the institution of mechanical engineers. Part A: J Power Energy 1994;208:1–12.
[6] Deng S, Jin H, Cai R, Lin R. Novel cogeneration power system with liquefied natural gas (LNG) cryogenic exergy utilization. Energy 2004;29:497–512.
[7] Krey G. Utilization of the cold by LNG vaporization with closed-cycle gas turbine. ASME J Eng Power 1980;102:225–30.
[8] Agazzani A, Massardo AF. An assessment of the performance of closed cycles with and without heat rejection at cryogenic temperatures. ASME J Eng Gas Turb Power 1999;121:458–65.
[9] Deng S, Jin H, et al. Novel gas turbine cycle with integration of CO_2 recovery and LNG cryogenic exergy utilization. In: Proceedings of ASME IMECE; 2001.
[10] Chiesa P. LNG receiving terminal associated with gas cycle power plants. ASME paper 97-GT-441; 1997.
[11] Desideri U, Belli C. Assessment of LNG regasification systems with cogeneration. In: Proceedings of TurboExpo 2000, Munich, Germany, 2000-GT-0165; 2000.
[12] Kim TS, Ro ST. Power augmentation of combined cycle power plants using cold energy of liquefied natural gas. Energy 2000;25:841–56.
[13] Velautham S, Ito T, Takata Y. Zero-emission combined power cycle using LNG cold. JSME Int J, Ser B. Fluids Therm Eng 2001;44:668–74.
[14] Riemer P. Greenhouse gas mitigation technologies, an overview of the CO_2 capture, storage and future activities of the IEA greenhouse gas R&D program. Energy Convers Manage 1996;37:665–70.
[15] Haugen HA, Eide LI. CO_2 capture and disposal: the realism of large scale scenarios. Energy Convers Manage 1996;37:1061–6.
[16] Jericha H, Gottlich E, Sanz W, Heitmeir F. Design optimization of the Graz cycle prototype plant. ASME J Eng Gas Turb Power 2004;126:733–40.
[17] Anderson R, Brandt H, Doyle S, Pronske K, Viteri F. Power generation with 100% carbon capture and sequestration. In: 2nd Annual conference on carbon sequestration, Alexandria, VA; 2003.
[18] Marin O, Bourhis Y, Perrin N, Zanno PD, Viteri F, Anderson R. High efficiency, zero emission power generation based on a high-temperature steam cycle. In: 28th International technical conference on coal utilization & fuel systems, Clearwater, FL, USA; 2003.
[19] Mathieu P, Nihart R. Zero-emission MATIANT cycle. J Eng Gas Turb Power 1999;121:116–20.
[20] Mathieu P, Nihart R. Sensitivity analysis of the MATIANT cycle. Energy Convers Manage 1999;40:1687–700.
[21] Zhang N, Lior N. A novel near-zero CO_2 emission thermal cycle with LNG cryogenic exergy utilization. Energy 2006;31:1666–79.
[22] Zhang N, Lior N. Proposal and analysis of a novel zero CO_2 emission cycle with liquid natural gas cryogenic exergy utilization. J Eng Gas Turb Power 2006;128:81–91.
[23] Ishida M, Jin H. CO_2 recovery in a novel power plant system with chemical-looping combustion. J Energy Convers Manage 1997;38(19):187–92.
[24] Ishida M, Jin H. A new advanced power-generation system using chemical-looping combustion. Energy – Int J 1994;19:415–22.
[25] Griffin T, Sundkvist SG, Asen K, Bruun T. Advanced zero emissions gas turbine power plant. ASME J Eng Gas Turb Power 2005;27:81–5.
[26] Kvamsdal HM, Jordal K, Bolland O. A quantitative comparison of gas turbine cycles with CO_2 capture. Energy 2007;32:10–24.
[27] Zhang N, Lior N, Liu M, Han W. COOLCEP (cool clean efficient power): novel CO_2-capturing oxy-fuel power systems with LNG (liquefied natural gas) coldness energy utilization, ECOS 2008. In: 21st Conference on efficiency, costs, optimization, simulation and environmental aspects of energy systems, vol. II, Krakow, Poland; 2008. p. 543–50.
[28] Liu M, Lior N, Zhang N, Han W. Thermoeconomic optimization of COOLCEP-S: a novel zero-CO_2-emission power cycle using LNG (liquefied natural gas) coldness. In: ASME paper IMECE2008-6467, Proc. IMECE2008, ASME international mechanical engineering congress and exposition, Boston, Massachusetts, ASME, NY, November 2–6; 2008.
[29] Aspen Plus®, Version 11.1, Aspen Technology, Inc. <http://www.aspentech.com/>.
[30] Lior N, Zhang N. Energy, exergy, and second law performance criteria. Energy – Int J 2007;32:281–96.
[31] Larson ED, Ren T. Synthetic fuel production by indirect coal liquefaction. Energy Sustain Dev 2003;VII(4).
[32] Kreutz T, Williams R, Consonni S, Chiesa P. Co-production of hydrogen, electricity and CO_2 from coal with commercially ready technology. Part B: Econ Anal Hydrogen Energy 2005;30:769–84.

[33] Jiaji Fu, Tong Yunhuan. Industrial economics. Beijing: Tsinghua University Press; 1996 [in Chinese].
[34] <http://www.wj.sh.cn/> [accessed October 2008].
[35] <http://www.kfas.com.cn/> [accessed October 2008].
[36] <http://www.cnjssw.com/> [accessed October 2008].
[37] <http://www.sunplushtech.com/low-temperature-pump.htm> [accessed October 2008].
[38] Hewitt GF, Shires GL, Bott TR. Process heat transfer. Boca Raton: CRC Press/Begell House; 1993.